Simulation of the Next-CSP Solar Loop Including a Hybrid Gas Turbine

Benjamin Grange[1, a)], Alex Le Gal[1] and Gilles Flamant[1]

[1]PROMES-CNRS, 7 rue du Four Solaire, 66120 Font-Romeu-Odeillo-Via, France.

[a)]benjamin.grange@promes.cnrs.fr

Abstract. The Next-CSP project aims at installing and demonstrating a complete collection and conversion solar loop using particle as heat transfer fluid and storage medium. It includes a pilot scale fluidized particles-in-tube solar receiver, two storage tanks, an air/particles heat exchanger and a hybrid solar gas turbine. A model of the complete system based on a modular approach is presented in this paper. It includes the simulation of the solar field, the solar receiver, the heat exchanger and the gas turbine. Each model is explained and results are presented during Equinox day. Performance of the different components are observed and discussed.

INTRODUCTION

The Next-CSP project [1] aims at demonstrating at pilot-scale the concept of CSP particle technology using high temperature particles as heat transfer fluid and storage medium. The system is installed at the Themis tower in Targasonne (France) and is operated by PROMES-CNRS. The solar receiver consists in a multi-tube absorber and a half cavity made of refractory panels. A refractory panel is also installed behind the tubes to reflect the concentrated radiation passing through the tube spacings. The fluidized particles flow upward in forty 3m-long tubes before flowing out in a hot storage tank. Then, the hot particles fall into a multi-staged fluidized bed heat exchanger to preheat the pressurized air exhausting from the compressor of a hybrid gas turbine. Figure 1 presents the design of the solar receiver as well as the layout of the Next-CSP facility.

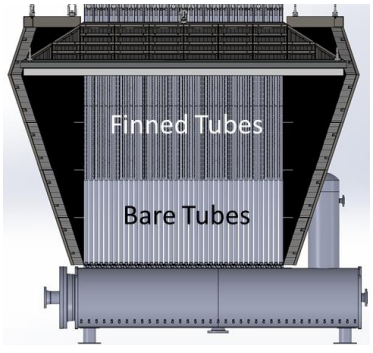

(a)

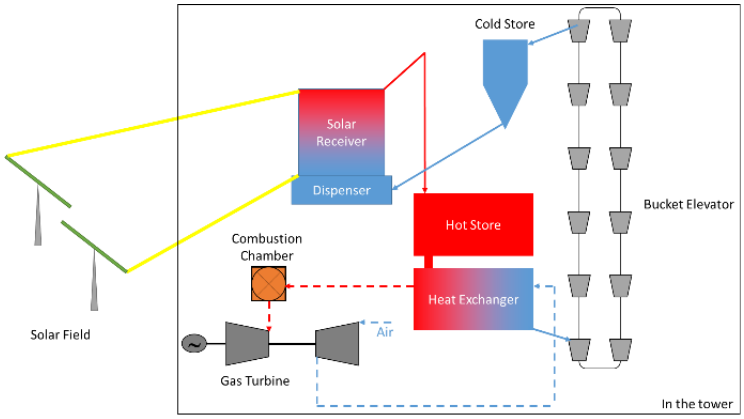

(b)

FIGURE 1. (a) Design of the solar receiver – (b) Layout of the Next-CSP facility installed at the Themis tower – Particles in solid lines, Air in dotted lines

SIMULATION OF THE COMPLETE SYSTEM

This section describes the method to simulate each component of the system: the solar field, the solar receiver, the heat exchanger (HEX) and the gas turbine (GT). It was used to simulate the performance of a medium-scale particle CSP plant driving a combined cycle [2].

Solar Field

The simulation of the solar field consists in an aiming point strategy (APS) in order to spread the concentrated solar flux on the forty tubes. It decreases the risk of hot spots appearance leading to receiver damage and offers more uniform particle temperature in the tubes. The aiming point strategy is achieved using the TABU search associated with the convolution-projection model UNIZAR [3]. An objective normalized flux distribution is defined using a Gaussian distribution horizontally and a normalized surge function vertically. Figure 2 shows a typical objective normalized flux distribution defined at mid-plane of the tubes. The ultimate goal is to keep the flux density on the tubes below 500 kW/m².

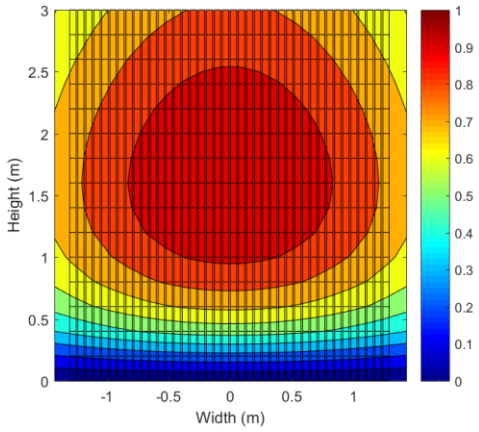

FIGURE 2. Typical objective normalized flux distribution

A grid of 5 x 5 aiming points is defined, each of the aiming point being separated horizontally and vertically 60 cm from each other. The cost function is the root-mean-square deviation between an objective normalized flux distribution and the normalized simulated flux distribution.

The aiming point of each heliostat is introduced into Solstice, a new open-source ray-tracing software developed by the CNRS-PROMES laboratory and Meso-Star SAS [4]. This simulation takes into account the tubular geometry of the solar receiver and the cavity panels surrounding it. Figure 3 shows a typical results delivered by Solstice and displayed in ParaView. The maximum flux density in this example is 440 kW/m² and the power at the aperture is 3 MW.

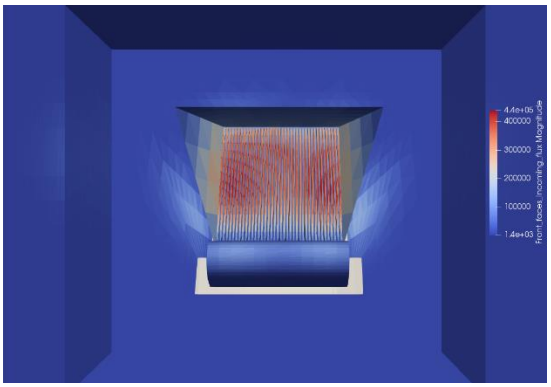

FIGURE 3. Results of ray-tracing software Solstice – Interface with ParaView

Solar Receiver

The flux distributions on the tubes and the cavity elements computed by Solstice are post-processed and implemented in a simplified thermal model developed with the Matlab® software [5]. Each tube is discretized by distinguishing the front and the back, and by dividing the height into 15 elements of 20 cm height. It results in 1200 elements for the tubes (30 elements per tube) and 104 additional elements for the cavity. The thermal model is based on the Net Radiation Method, which makes the balance on heat flux and radiosity. The view factor between each element is calculated. The tubes are made of Stainless Steel 310S and are painted with Pyromark 2500. The maximum temperature allowed is 900°C. The cavity and the back panel are made of ALSIFLEX® 1260.

Table 1 provides the optical properties of the Pyromark and of the ALSIFLEX® 1260.

TABLE 1. Optical properties of Pyromark 2500 and ALSIFLEX® 1260

Optical property	Pyromark 2500	ALSIFLEX® 1260
Solar Absorptance α (-)	0.9	0.2
Emissivity ε (-)	0.85	0.93

Figure 4 shows typical results computed by the thermal model.

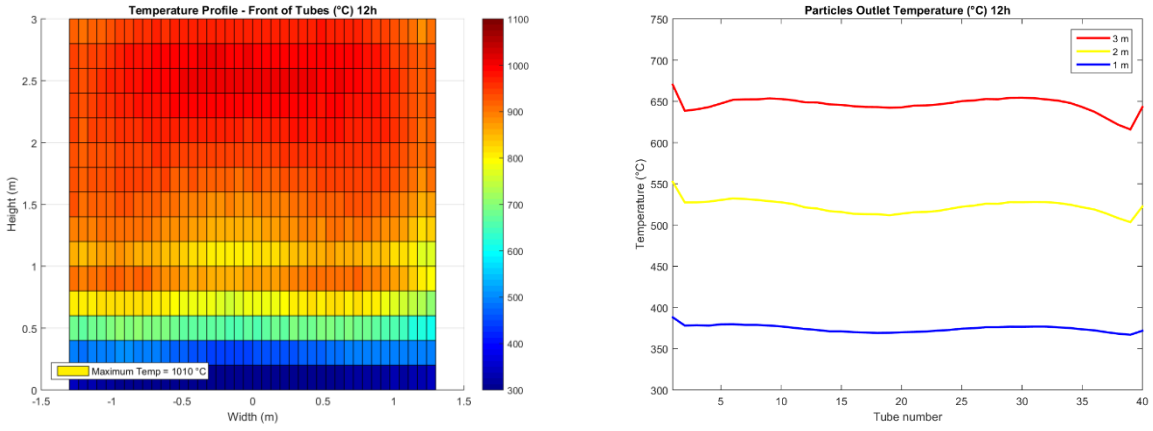

(a) (b)

FIGURE 4. (a) Temperature profile of the front of the tubes – (b) Particle temperature at 1 m, 2 m and 3 m height in the tubes

In this example, the maximum wall temperature is higher than the one allowed (Fig. 4.a), however it can be reduced by decreasing the number of operating heliostat. Figure 4.b shows that the particle temperature in all the tubes is rather uniform, hence validating the effectiveness of the APS.

Heat Exchanger

The particle temperature computed by the thermal model is introduced into the multi-stage tube/shell HEX model [6]. The compressed air coming from the Gas Turbine (GT) flows in the 1400 tubes in counter-current with the particles that are fluidized through six stages. The energy balance on one stage of a fluidized bed HEX is:

$$\dot{Q}_{particles} = \dot{Q}_{working\_air} + \dot{Q}_{fluidizing\_air} \tag{1}$$

2% of the particle power is assumed to go into the fluidizing air, therefore:

$$\dot{Q}_{fluidizing\_air} = 0.02 \times \dot{Q}_{working\_air} \tag{2}$$

The heat released by the particles can be calculated as follow:

$$\dot{Q}_{particles} = \pi . D_{tube\_outer} . h_{particles} . \left(T_{particles} - T_{tube\_outer}\right) \tag{3}$$

And

$$\dot{Q}_{particles} = \dot{m}_{particles} . c_{p,particles} \left(T_{particles,in} - T_{particles,out}\right) \tag{4}$$

Similarly, the heat gained by the working air can be expressed:

$$\dot{Q}_{working\_air} = \pi . D_{tube\_inner} . h_{working\_air} . \left(T_{tube\_inner} - T_{working\_air}\right) \tag{5}$$

And

$$\dot{Q}_{particles} = \dot{m}_{working\_air} . c_{p,working\_air} \left(T_{working\_air,out} - T_{working\_air,in}\right) \tag{6}$$

A heat transfer coefficient $h_{particles}$ of 800 W/m².K is considered between the fluidized particles and the tubes. The Gnielinski correlation [7] is applied to calculate the heat transfer coefficient $h_{working\_air}$ between the working air and the tubes:

$$Nu_{working\_air} = \frac{\left({F_{friction}}/{8}\right).(Re-1000).Pr}{1+12.7\sqrt{(F_{friction}/8}.\left(Pr^{\frac{2}{3}}-1\right)} \left(\frac{Pr}{Pr_{tube}}\right)^{0.11} \tag{7}$$

With $F_{friction}$ calculated as follow:

$$F_{friction} = (1.82 \times \log_{10}(Re) - 1.64)^{-2} \tag{8}$$

The inner and outer tube temperatures are assumed equal.
An algorithm simulating the six stages of the HX gives the inlet/outlet and air/particle temperatures in each stage. Figure 5 shows a typical results of the simulation.

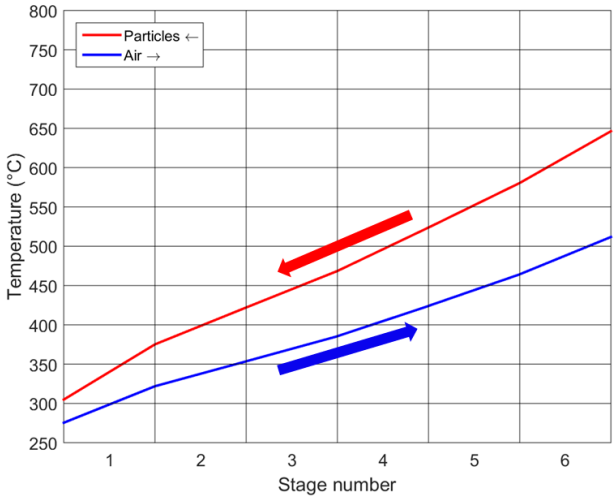

FIGURE 5. Air and particles temperature in the six stages of the fluidized bed HEX

The outlet gas temperature is limited by the heat transfer coefficient between the tubes and the working air (~200 W/m².K). A better design (smaller tube diameter) can be achieved and would lead to higher air temperature.

Gas Turbine

Typical GT cycle consists of a compressor, a combustion chamber, and a turbine section. A practical technique, based on the performance maps of the turbine and compressor sections, is used to model the GT cycle. This approach enables to predict the turbine performance for part-load operations, based on similarity and dimensional analyses, and is widely used in turbomachinery [8]. For the compressor, the maps provide the compressor ratio and isentropic efficiency as a function of the corrected mass flow and corrected shaft speed. For the turbine section, the maps provide isentropic efficiency and expansion ratio as a function of the same parameters.

These corrected parameters include reference inlet pressure and temperature (15°C, 1 atm). For the compressor, the corrected shaft speed and the corrected mass flowrate are expressed as follow:

$$N_{cor\_C} = \frac{N_{rot}}{\theta_C} \tag{9}$$

$$\dot{m}_{cor\_C} = \dot{m}_{air}\frac{\theta_C}{\alpha_C} \tag{10}$$

θ_C and α_C are non-dimensional factors defined as:

$$\theta_C = \sqrt{\frac{T_{C,in}}{T_{ref}}} \tag{11}$$

$$\alpha_C = \frac{P_{C,in}}{P_{ref}} \tag{12}$$

The compression ratio and isentropic efficiency are function of these parameters. The following relation provides the air temperature at the outlet of the compressor for isentropic process:

$$T_{C,out,is} = T_{C,in}(\delta_C)^{\frac{\gamma_C - 1}{\gamma_C}} \tag{13}$$

Calculating the actual outlet temperature of the compressor is carried out by applying the isentropic efficiency definition:

$$\eta_{C,is} = \frac{h_{C,out,is} - h_{C,in}}{h_{C,out} - h_{C,in}} \tag{14}$$

The turbine section is modeled using the same method. An iteration process determines the compressor mass flow rate and the fuel mass flow rate. Figure 6 presents typical results of the GT.

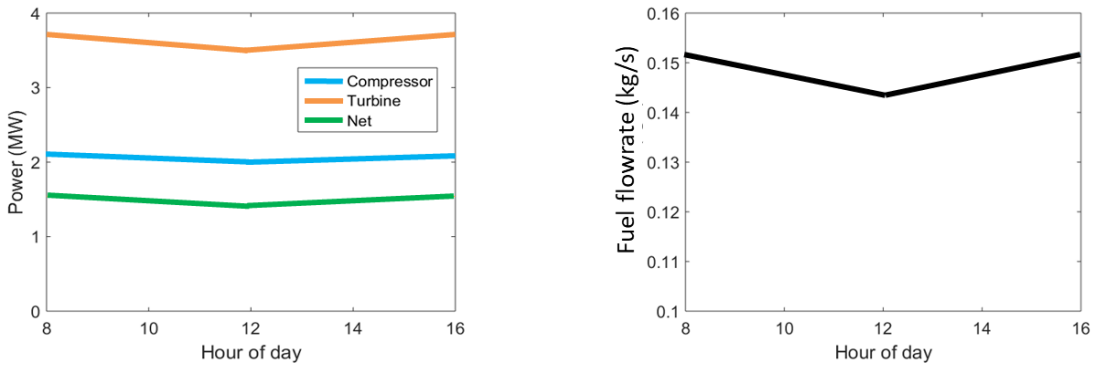

(a) (b)

FIGURE 6. (a) Power consumed by the compressor, power produced by the turbine and net power during the day – (b) Fuel consumption during the day

In the hybrid gas turbine, the air entering the combustion chamber is at the temperature of the last HEX stage, tube side. The convergence is the same as in the GT model expect that one more iteration loop is added. Indeed the outlet particle temperature of the solar receiver has to be equal to the inlet particle temperature of the HEX (neglecting the losses in the hot store), and the inlet particle temperature of the solar receiver has to be equal to the outlet particle temperature of the HEX (neglecting the heat losses in the bucket elevator).

RESULTS

Combining the different components model presented in the sections above results in determining all the required parameters to assess the performance of the system, such as the optical/thermal efficiency, the air and particle temperature in each component or the fuel consumption. Simulations are carried out at Equinox, the DNI considered and the power at the aperture of the receiver are shown in Fig. 7.

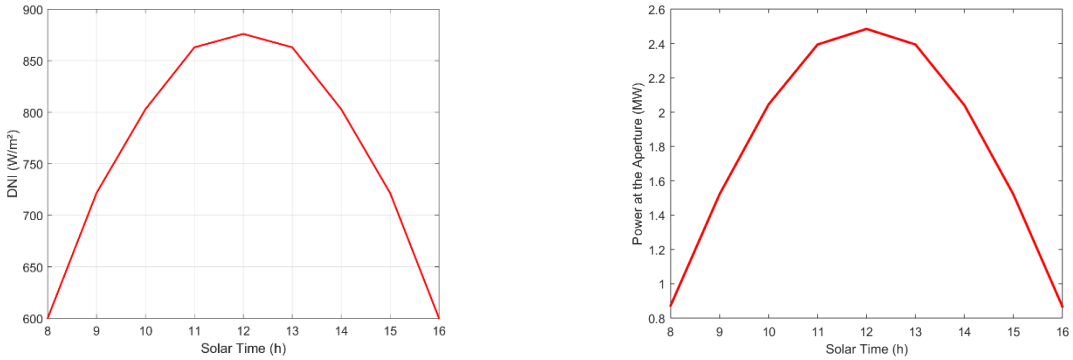

(a) (b)

FIGURE 7. (a) DNI evolution during the Equinox – (b) Evolution of the power at the aperture of the receiver during the day

Figure 8 shows some results computed by the hybrid solar GT model.

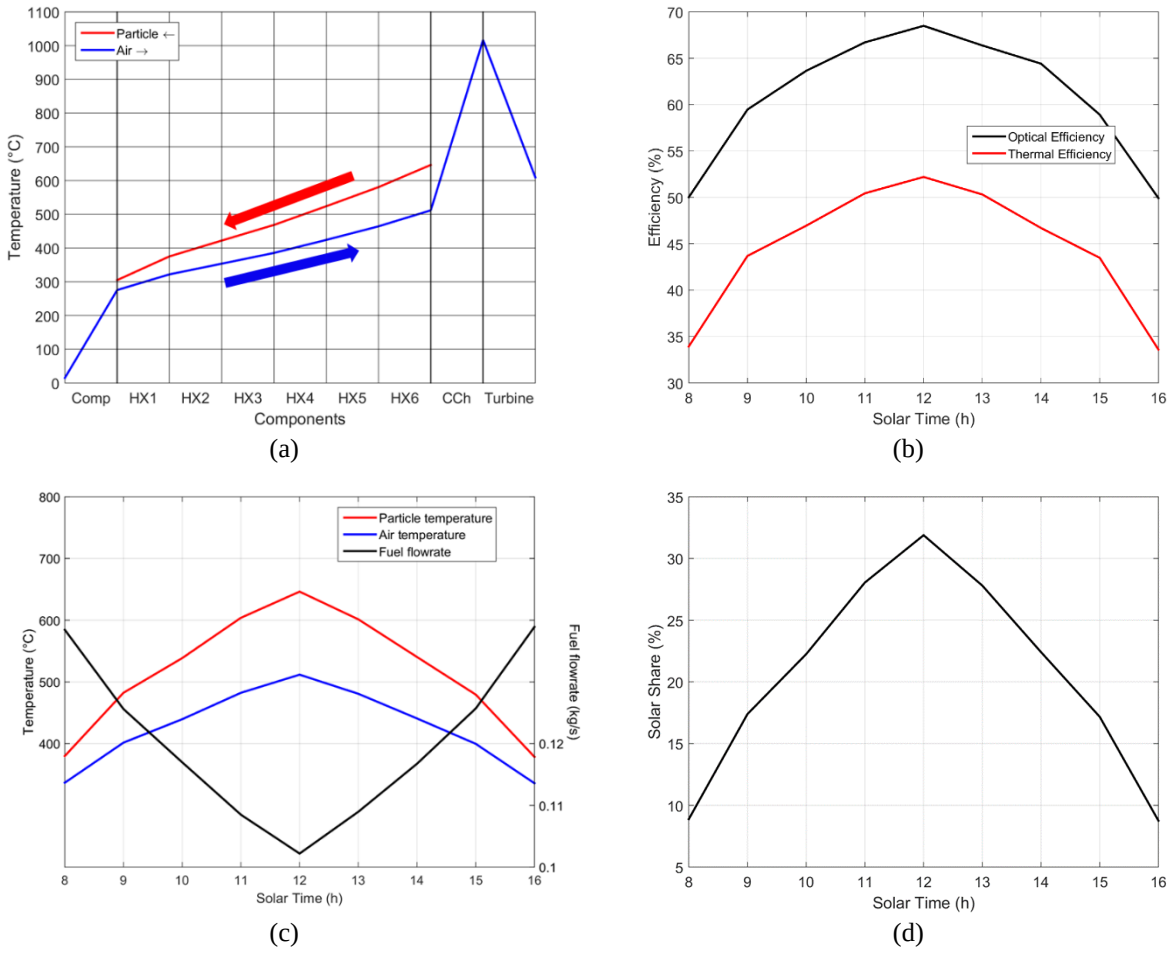

FIGURE 8. (a) Air/Particle temperature in the system at noon – (b) Optical end thermal efficiency during the day – (c) Air/Particle temperature at the outlet/inlet of the HX and fuel consumption during the day – (d) Solar share during the day

The optical and thermal efficiency varies from 50% to 68.5% and from 34% to 52.2%, respectively. The low thermal efficiency of the solar receiver is due to the layout of the existing Themis solar field not optimized for the fluidized bed solar receiver.

During the day, the particle temperature at the outlet of the solar receiver varies from 380°C to 650°C, resulting in an air temperature at the outlet of the HEX from 340°C up to 520°C. The fuel required to reach the TIT ranges between 102 g/s and 139 g/s. The resulting solar share varies from 8% to 32%.

DISCUSSION

The value presented in the previous section are relatively low. The reason is that the complete system is not optimized because the main objective of the project is to operate the particle loop at large pilot scale (Until now, it was demonstrated at 150kW-scale [9]) and to demonstrate the coupling with the gas turbine whatever the efficiencies. As abovementioned, the solar field layout is not adapted to the solar receiver. Moreover, the design of the heat exchanger is not optimized due to cost issues, leading to a very low heat transfer coefficient between the working air and the tubes. Finally and most importantly, the GT is a commercial engine [10] that was solarized to be adapted to the particle loop. As a result, the turbine inlet temperature (TIT), approximately 1000°C, is by far too high to reach high solar share. The capacity of the concept to reach high efficiency and high solar share is demonstrated in [2].

ACKNOWLEDGMENTS

This project has received funding from the European Union's Horizon 2020 research and innovation program under grant agreement No 727762, project acronym NEXT-CSP.

This work was supported by the French "Investments for the future" program managed by the National Agency for Research, under contract ANR-10-EQPX-49-SOCRATE (Equipex SOCRATE).

REFERENCES

1. http://next-csp.eu/.
2. Behar et al. Energy Conversion and Management 220, 113108 (2020).
3. F.J. Collado et al., Journal of Solar Energy 37, 215-234 (1986).
4. PROMES-CNRS, MESO-STAR SAS. SOLSTICE, SOLar Simulation Tool In ConcEntrating optics, version 0.7.1 (2017), France, https://www.meso-star.com/projects/solstice.html https://www.labex-solstice.fr/logiciel-solstice.html.
5. B. Grange et al., Journal of Solar Energy Engineering 133(3), 031004 (2011).
6. F. Gomez-Garcia et al., Applied Energy 190, 510-523 (2017).
7. Çengel Y., Cimbala J.M. Fluid Mechanics Fundamentals and Applications. McGraw-Hill College, 2017, ISBN:1259696537.
8. Dixon S.L., Hall C.A. Fluid Mechanics and Thermodynamics of Turbomachinery. Sixth edition, Butterworth-Heinemann, 2014.
9. Perez-Lopez I. et al. Solar Energy 137, 463–476 (2016).
10. https://www.opraturbines.com/gas-turbine/